

# Nature and Origin of the Brucejack High-Grade Epithermal Gold Deposit, Northwestern British Columbia (NTS 104B): 2017 Update

**D.F. McLeish**, Department of Earth and Planetary Sciences, McGill University, Montréal, QC, [duncan.mcleish@mail.mcgill.ca](mailto:duncan.mcleish@mail.mcgill.ca)

**A.E. Williams-Jones**, Department of Earth and Planetary Sciences, McGill University, Montréal, QC

**W.S. Board**, Pretium Resources Inc., Vancouver, BC

**J.R. Clark**, Department of Earth and Planetary Sciences, McGill University, Montréal, QC

---

McLeish, D.F., Williams-Jones, A.E., Board, W.S. and Clark, J.R. (2018): Nature and origin of the Brucejack high-grade epithermal gold deposit, northwestern British Columbia (NTS 104B): 2017 update; *in* Geoscience BC Summary of Activities 2017: Minerals and Mining, Geoscience BC, Report 2018-1, p. 31–40.

## Introduction

The Brucejack Au-Ag deposit of Pretium Resources Inc. (MINFILE 104B 193 and 104B 199; BC Geological Survey, 2017) is a recently discovered, large and exceptionally high grade (up to 41 000 g/ton Au), intermediate- or possibly low-sulphidation, epithermal deposit located in the Stewart–Eskay Creek mining district of northwestern British Columbia (BC). With commissioning completed in May of 2017 and commercial production achieved two months later, the deposit is host to Canada’s newest Au mine. This project is taking advantage of the unparalleled opportunity offered by the extensive preproduction exploration and mine-development workings at Brucejack to study the genesis and evolution of high-grade epithermal Au deposits and, in particular, investigate 1) the chemical (including isotopic) characteristics of its ores and associated hydrothermal alteration; 2) the general mechanisms responsible for high-grade Au transport at temperatures characteristic of the epithermal realm; 3) the physicochemical conditions controlling Au deposition during the different stages of mineralization; and 4) the genetic relationship with spatially associated porphyry systems (if any). Ultimately, the aim of the project is to address the fundamental question of whether the large, high-grade Brucejack resource can be explained using a simple solubility model.

This paper provides an update on the study and presents findings made since the initial project overview was published last year (McLeish et al., 2017). Specific attention is given to recent advances in understanding the different styles of Au mineralization in the deposit, including the recent discovery of invisible Au mineralization in arsenian pyrite, as well as progress made in other areas of ore- and alteration-mineral chemistry. The problem of low-tempera-

ture Au solubility in hydrothermal fluids, a major motivation for this project, is discussed at length in the McLeish et al. (2017) paper and is not repeated here; the interested reader is referred to the ‘Introduction’ section of that paper for more information. The regional and property geology descriptions and the deposit mineralization overview are repeated from McLeish et al. (2017), with minor updates to deposit geochronological and lithostratigraphic data.

## Regional Geology

The Brucejack deposit is situated in the northwestern Stikine terrane (Figures 1, 2), a paleo-island arc system akin to that of the modern-day Philippine archipelago (Marsden and Thorkelson, 1992). The Stikine terrane formed as an intraoceanic island arc in the mid-Paleozoic and was accreted to the western continental margin of Laurentia in the Middle to Late Jurassic (Monger et al., 1991; Anderson, 1993). Volcano-sedimentary rocks of the Late Triassic Stuhini Group and Early Jurassic Hazelton Group dominate the stratigraphy of the Stikine terrane. Two distinct episodes of magmatism in the Late Triassic and in the Early Jurassic (229–221 Ma and 195–175 Ma, respectively; Macdonald et al., 1996) affected the Stuhini-Hazelton succession, which was deformed during Middle to Late Jurassic accretion and later Cretaceous compressional tectonism (Greig and Brown, 1990; Alldrick, 1993). Porphyry magmatism is known to have spanned the interval ca. 220–186 Ma on a terrane scale (Logan and Mihalynuk, 2014); however, within the Stewart–Eskay Creek district, U-Pb ages for porphyry intrusions are generally limited to the ca. 197–193 Ma range (Kirkham and Margolis, 1995).

## Brucejack Property Geology

Five zones of mineralization have been explored in detail at Brucejack (West, Valley of the Kings, Bridge, Gossan Hill and Shore zones; Figure 3), all of which are hosted within hornblende- and/or feldspar-phyric volcanic flows, lapilli

---

*This publication is also available, free of charge, as colour digital files in Adobe Acrobat® PDF format from the Geoscience BC website: <http://www.geosciencebc.com/s/SummaryofActivities.asp>.*

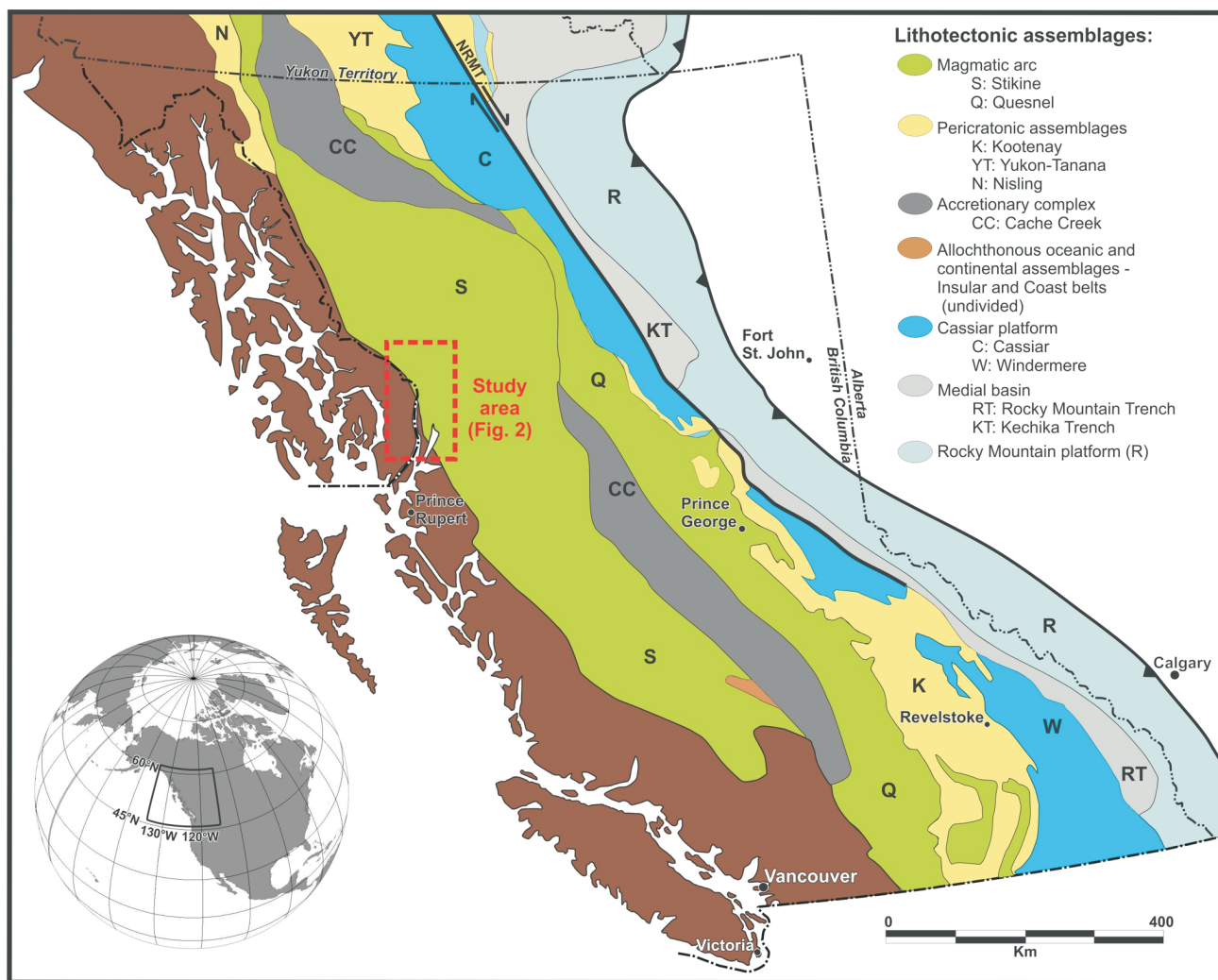


**Figure 1:** Location of the study area in reference to the major lithotectonic subdivisions of the Canadian Cordillera (modified after McLeish [2013] with lithotectonic boundaries from Johnston [2008]). Abbreviation: NRMT, Northern Rocky Mountain Trench (fault).

tuff, locally derived pyroclastic and volcanic conglomerate, and volcanic sandstone, siltstone and mudstone of the lowermost Hazelton Group, proximal to the regional-scale unconformity between the Stuhini and Hazelton groups (Board and McNaughton, 2013). To the immediate west and northwest of these zones, monzonitic, syenitic and granitic rocks of the Mitchell suite intruded volcanoclastic rocks of the Stuhini and Hazelton groups; these intrusions are closely associated with porphyry-style Cu-Au-Mo mineralization on the adjacent Kerr-Sulphurets-Mitchell and Snowfield properties (Kirkham and Margolis, 1995). Uranium-lead zircon ages from various phases of these intrusions suggest that the porphyry-style mineralization was emplaced at 197–190 Ma (Bridge, 1993; Margolis, 1993; Macdonald et al., 1996; Febbo et al., 2015). Large areas of hydrothermal alteration affected and surround the intrusive complexes of the Mitchell suite. These consist of 1) early potassic alteration closely associated with porphyry Cu and Au mineralization; 2) locally overprinting propylitic and chlorite-sericite alteration; and 3) widespread and well-de-

veloped, late quartz-sericite-pyrite alteration that pervasively overprinted earlier alteration and extends distally into the surrounding hostrocks of the Stuhini and Hazelton groups (Ghaffari et al., 2012).

### Deposit Mineralization

Within the Valley of the Kings zone (VOK; Figure 3), Au mineralization is hosted by extensive, predominantly sub-vertical, quartz-carbonate-sulphide vein stockworks and subordinate vein breccias. Five stages of veins have been recognized in the VOK: 1) discontinuous pyrite-stringer veins containing carbonate and quartz ( $V_{n0}$ ); 2) electrum-bearing quartz-carbonate±sericite sheeted, stockwork and brecciated veins ( $V_{n1a}$ ,  $V_{n1b}$  and  $V_{n1c}$ , respectively); 3) Zn–Pb±Cu sulphide veins containing Ag sulphosalts and electrum ( $V_{n2}$ ); 4) carbonate±quartz veins containing abundant orange-coloured, Mn-bearing calcite, and electrum ( $V_{n3}$ ); 5) postmineralization, Cretaceous, orogenic quartz±carbonate shear veins with rare, remobilized pyrite,

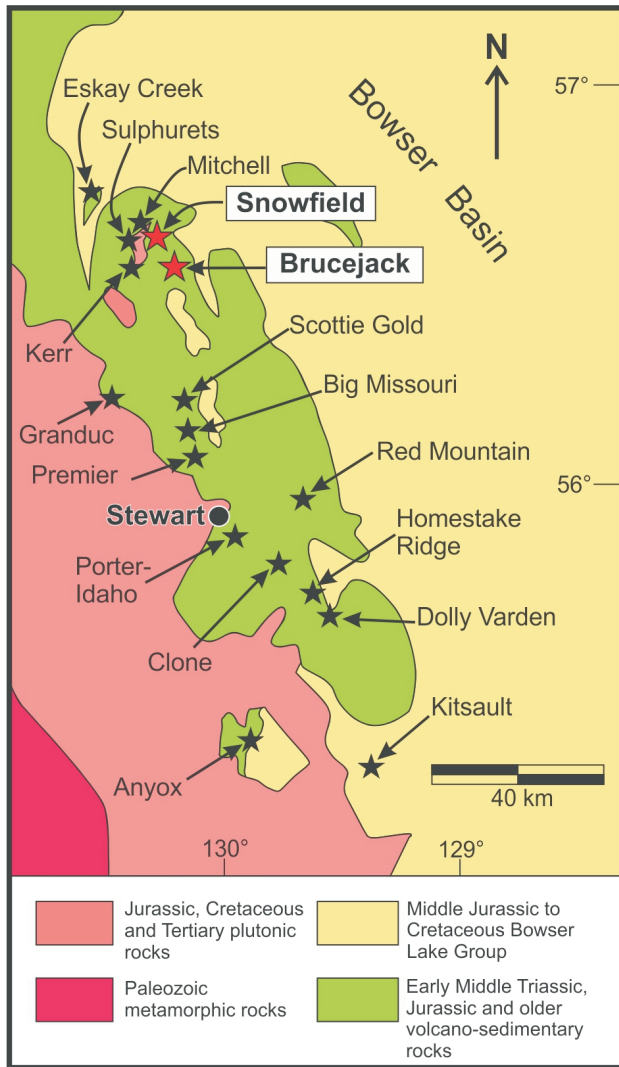


**Figure 2:** Major porphyry, epithermal and volcanogenic massive-sulphide deposits of the Stewart–Eskay Creek district (modified after Ghaffari et al., 2012), with the locations of the Brucejack and Snowfield properties highlighted.

electrum and base-metal sulphides in thrust-related shear bands ( $Vn_{4a}$ ,  $Vn_{4b}$ ) and subhorizontal, barren, white quartz tension-gash veins with adjacent chlorite alteration ( $Vn_{4c}$ ; classification modified after Tombe et al., 2014). The  $Vn_0$ ,  $Vn_{1a-c}$ ,  $Vn_2$  and  $Vn_3$  veins are largely undeformed to weakly deformed, except within localized strain zones where they are moderately to strongly deformed. Evidence from cross-cutting relationships paired with recent, unpublished, hostrock U-Pb zircon determinations have constrained the age of  $Vn_{1a-c}$ ,  $Vn_2$  and  $Vn_3$  vein formation to ca. 184–183 Ma (Board, pers. comm., 2017). Variably developed but generally intense quartz-sericite-pyrite alteration occurs throughout the deposit but is strongest proximal to the Brucejack fault and the unconformity between the Stuhini and Hazelton groups, which suggests that these structures may have acted as important fluid conduits during hydrothermal alteration and mineralization. Preliminary paleo-

temperature vectors derived from alteration, mineralization and vein textures suggest a down-temperature thermal gradient toward the east (up stratigraphy) and away from the Snowfield and Kerr-Sulphurets-Mitchell higher temperature porphyry centres, located northwest of the deposit (Board, 2014).

## Preliminary Mineral Chemistry

### Pyrite

Following the discovery of widespread, oscillatory zoned arsenian pyrite during the initial petrography study (McLeish et al., 2017), pyrite from all mineralization-stage vein types ( $Vn_{1s}$ ,  $Vn_2$  and  $Vn_3$ ) was analyzed using electron microprobe analyzer–wavelength dispersive spectroscopy (EMPA-WDS). The goal of these analyses was to determine if the arsenian pyrite hosts any invisible Au mineralization, either as submicroscopic ( $<0.1 \mu\text{m}$ ) crystal inclusions or as Au atoms structurally bound in the pyrite lattice (i.e., in solid solution), as has been found in other epithermal deposits (e.g., Reich et al., 2005). Two representative arsenian-pyrite-bearing thin sections from each vein class were chosen for study based on the nature of the oscillatory zoned arsenian pyrite, which was determined by backscattered-electron (BSE) imaging.

The EMPA-WDS analyses of pyrite were performed at the joint University of Ottawa–Canadian Museum of Nature MicroAnalysis Laboratory using a JEOL 8230 SuperProbe with five X-ray wavelength-dispersive spectrometers. Pyrite grains from 18 thin sections were quantitatively analyzed for As ( $L\alpha$ ), Au ( $L\alpha$ ), Cu ( $K\alpha$ ), Fe ( $K\alpha$ ), and S ( $K\alpha$ ) using the following synthetic and natural standards: Au80Ag20 alloy (Au), cubanite (Cu), GaAs alloy (As) and pyrite (Fe and S). Microbeam analyses were performed using a beam energy of 20 keV, a  $40^\circ$  takeoff angle, a  $2 \mu\text{m}$  beam diameter and a 200 nA beam current. Minimum detection limits of 150 ppm and 100 ppm Au were achieved using these operating conditions with 100 and 200 second counting times, respectively.

Results from BSE imaging and EMPA-WDS analyses show oscillatory zoned arsenian pyrite contains localized occurrences of high-grade Au mineralization (150–1920 ppm Au; Figure 4). Many of the pyrite grains analyzed contain electrum-filled fractures that clearly crosscut the As-bearing oscillatory zones (Figure 4a, b), indicating that pyrite-hosted invisible Au mineralization predates electrum-stage mineralization. Furthermore, phyllically altered wallrocks in the VOK host oscillatory zoned pyrite similar to that documented in all three mineralization-stage vein types (cf. Figure 5, grains S430136a and U585EX315). This suggests that the vein-hosted pyrite may be inherited from the wallrocks. Pre-electrum deformation of pyrite is also locally evident in the form of microfractures offsetting

arsenian growth zones in the intermediate sections of grains (Figure 4c).

In order to better understand the distribution of Au and other trace elements in VOK pyrite, laser-ablation inductively coupled plasma–mass spectrometry (LA-ICP-MS) maps of pyrite were prepared. Although destructive and having less spatial resolution than the EMPA-WDS method, LA-ICP-MS has the advantage of being able to provide multi-element data rapidly for an entire mineral grain. Twenty-eight pyrite grains with oscillatory, As-rich growth zones were selected for LA-ICP-MS mapping. All grains chosen were hosted completely within, or were immediately adjacent to,  $Vn_1$  or  $Vn_3$  veins.

Sixteen grains were successfully mapped using a Resonetics RESOLUTION M-50 ArF excimer laser (193 nm) coupled to an Agilent 7900x ICP-MS at the Laboratoire des Matériaux Terrestres of the l'Université du Québec à Chicoutimi. The concentrations of  $^{27}\text{Al}$ ,  $^{29}\text{Si}$ ,  $^{33}\text{S}$ ,  $^{34}\text{S}$ ,  $^{44}\text{Ca}$ ,  $^{47}\text{Ti}$ ,  $^{51}\text{V}$ ,  $^{53}\text{Cr}$ ,  $^{55}\text{Mn}$ ,  $^{57}\text{Fe}$ ,  $^{59}\text{Co}$ ,  $^{60}\text{Ni}$ ,  $^{61}\text{Ni}$ ,  $^{63}\text{Cu}$ ,  $^{65}\text{Cu}$ ,  $^{66}\text{Zn}$ ,  $^{72}\text{Ge}$ ,  $^{74}\text{Ge}$ ,  $^{75}\text{As}$ ,  $^{77}\text{Se}$ ,  $^{82}\text{Se}$ ,  $^{95}\text{Mo}$ ,  $^{96}\text{Mo}$ ,  $^{109}\text{Ag}$ ,  $^{111}\text{Cd}$ ,  $^{113}\text{In}$ ,  $^{115}\text{In}$ ,  $^{118}\text{Sn}$ ,  $^{121}\text{Sb}$ ,  $^{125}\text{Te}$ ,  $^{128}\text{Te}$ ,  $^{137}\text{Ba}$ ,  $^{182}\text{W}$ ,  $^{184}\text{W}$ ,  $^{197}\text{Au}$ ,  $^{200}\text{Hg}$ ,  $^{202}\text{Hg}$ ,  $^{203}\text{Tl}$ ,  $^{204}\text{Pb}$ ,  $^{205}\text{Tl}$ ,  $^{206}\text{Pb}$ ,  $^{207}\text{Pb}$ ,  $^{208}\text{Pb}$  and  $^{209}\text{Bi}$  were measured. Element-distribution maps (Figure 5) were made by performing a series of line scans across each grain with a beam size of 11–19  $\mu\text{m}$  and a stage speed of 10–20  $\mu\text{m/s}$ . A laser fluence of 13  $\text{J/cm}^2$  with a repetition rate of

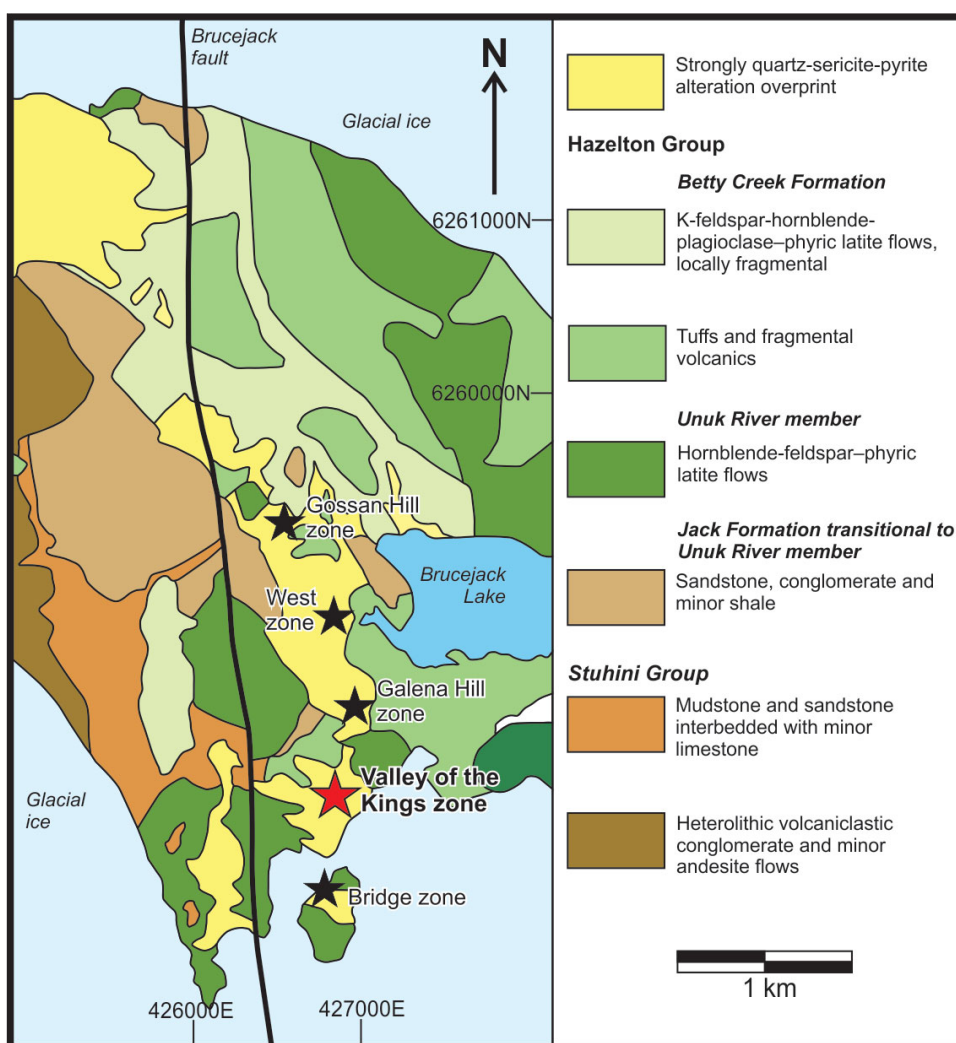


**Figure 3:** Geology of the Brucejack deposit area (modified after Tombe [2015] with revised stratigraphic nomenclature from Nelson and Kyba [2014]), showing five main zones of mineralization that are hosted within a moderately to strongly sericite-quartz-pyrite-altered sequence of hornblende- and/or feldspar-phyrlic volcanic flows, lapilli tuffs, locally derived pyroclastic and volcanic conglomerate, and volcanic sandstone, siltstone and mudstone of the lowermost Hazelton Group. All zones are proximal to a regional-scale unconformity between the Stuhini and Hazelton groups. Area covered by this figure is approximately the size of Brucejack star on Figure 1.

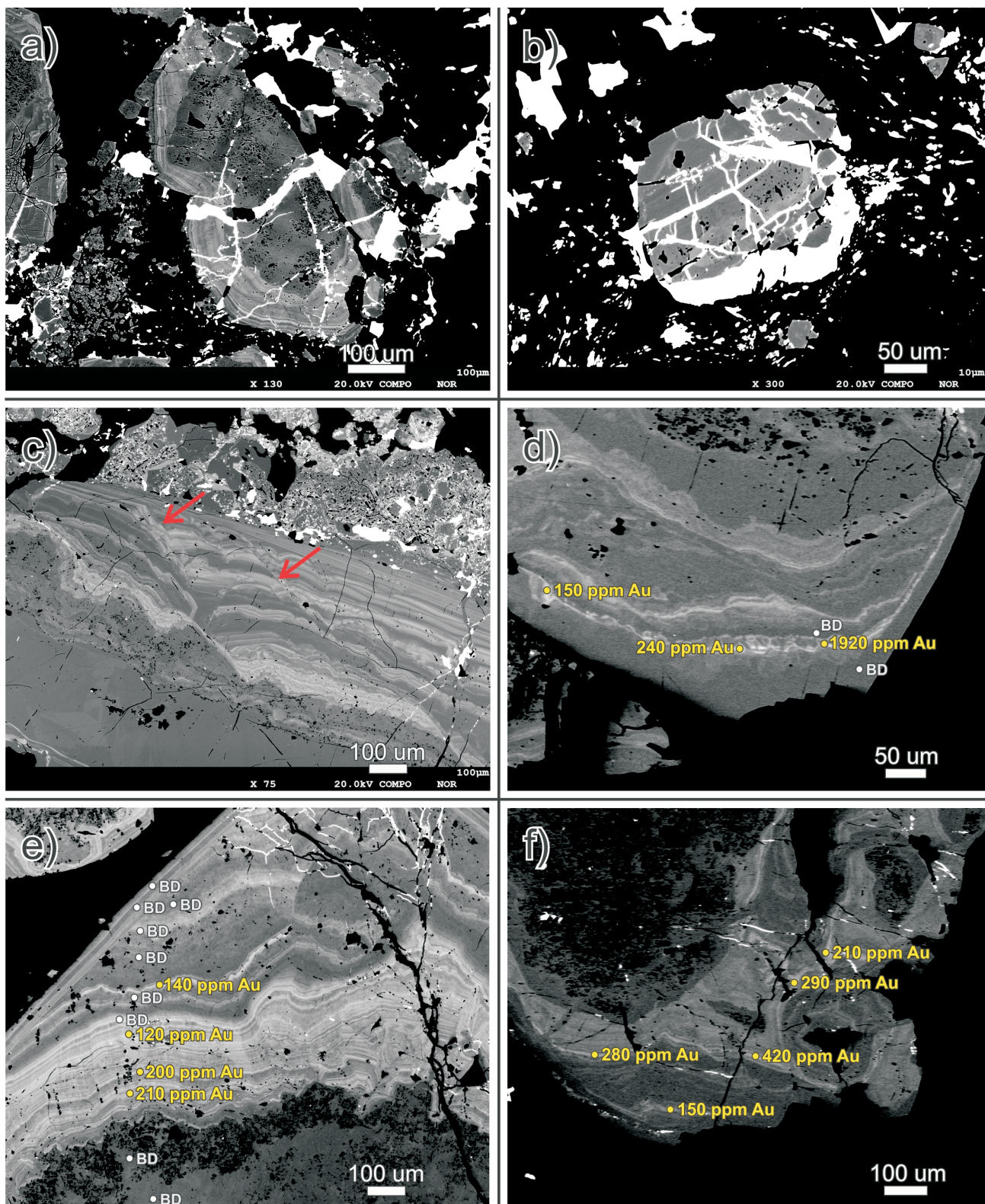


**Figure 4:** Backscattered-electron (BSE) images of pyrite and electrum from ore-stage quartz-carbonate veins at the Brucejack deposit: **a) and b)** electrum (brightest mineral) crosscuts oscillatory zoned arsenian pyrite (As-rich bands of pyrite are lighter coloured and surround an As-poor pyrite core); **c)** pre-electrum deformation of the arsenian pyrite is manifested by several groups of microfractures (red arrows) in the pyrite, which offset intermediate arsenian pyrite bands but do not propagate into the outermost pyrite growth zones; **d), e)** and **f)** EMPA-WDS spot analyses of pyrite indicate significant Au concentrations in irregularly shaped, intermediate, arsenian growth zones (yellow dots), whereas As-poor cores and outer growth zones all have Au concentrations below detection limit (grey dots labelled 'BD'; i.e., <100 ppm Au).

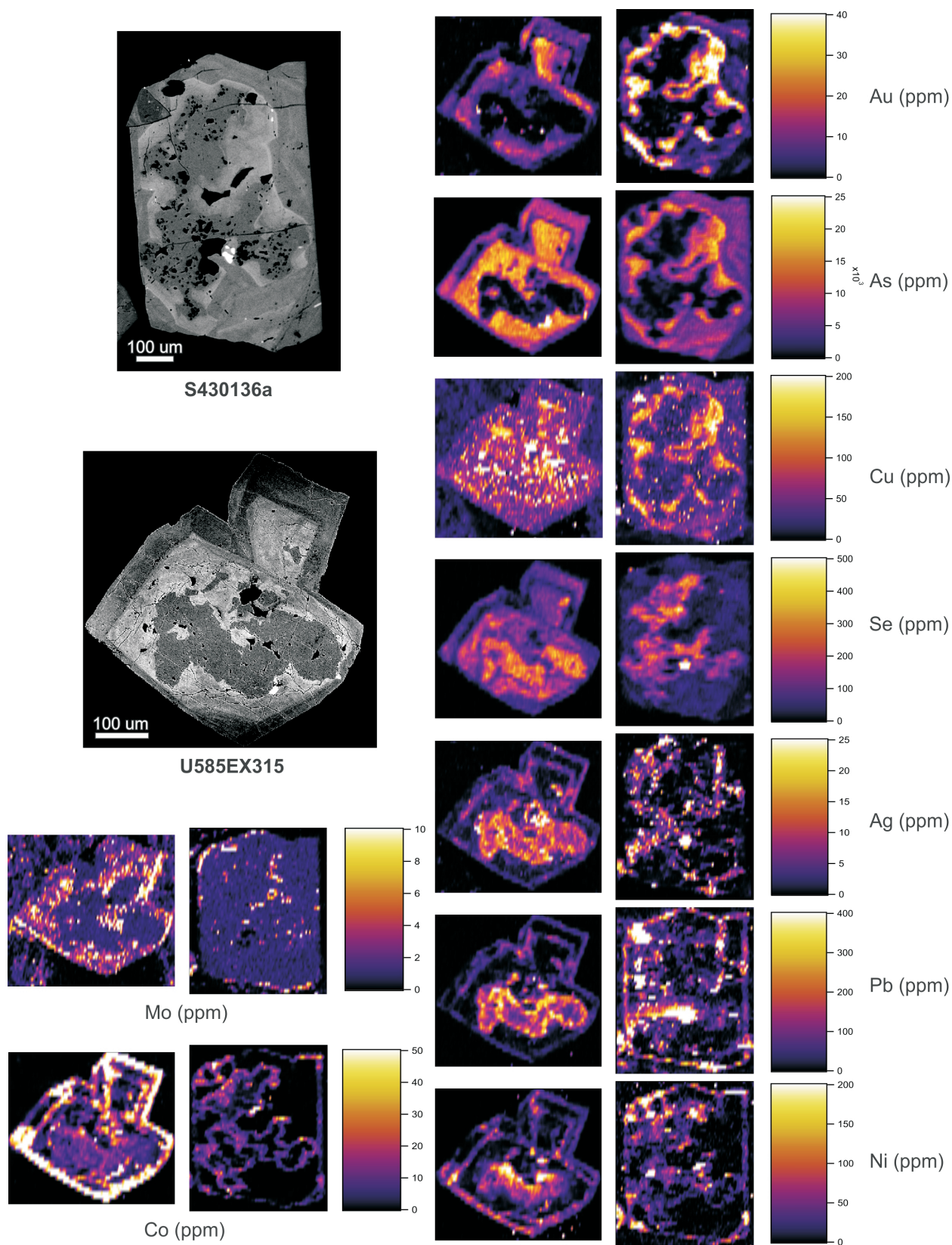


**Figure 5:** Laser-ablation inductively coupled plasma–mass spectrometry (LA-ICP-MS) elemental maps of pyrite from the Valley of the Kings zone at the Brucejack deposit, shown in reference to the grain before ablation (BSE images at top left). The upper BSE image is of a pyrite grain from a sample containing ore-stage ( $Vn_1$ ) vein-hosted pyrite (sample S430136a). The lower BSE image is of a pyrite grain from a sample containing medium- to coarse-grained, wallrock-hosted pyrite located marginal to a  $Vn_1$  vein (~1 cm away from the vein margin; sample U585EX315). See text for discussion.

15 Hz was used for all line scans. The following certified standards were used for external calibration: JB-MSS5, a synthetic FeS crystal, containing 50–70 ppm of most chalcophile elements, supplied by J. Brenan of Dalhousie University; MASS-1, a ZnCuFeS pressed-powder pellet doped with 50–70 ppm of Ag, As, Bi, Pb, Re, Sb, Se, Sn and Te, supplied by the United States Geological Survey (USGS); Laflamme Po727, a synthetic FeS crystal doped with 40 ppm of platinum-group elements and Au, supplied by Memorial University; and GSE-1G, a synthetic glass doped with 300–600 ppm Ba, Cr, Ge, La, Mn, Ni, Re, Si, Sr, Ti, V, W and Yb, supplied by the USGS. The standard JB-MSS5 was also used as a secondary reference material for intrastandard quality control. The maps were generated in the software package Iolite using the time-resolved composition of each element; they are semiquantitative and indicate the relative concentration of each element.

Preliminary results from LA-ICP-MS mapping of characteristic VOK vein-hosted, and wallrock-hosted vein-marginal, pyrite are presented in Figure 5. These grains generally display similar trace-element distribution patterns, with several elements being strongly zoned. The elements Se, Sb, Ni, Pb, Ag, and Bi are strongly focused in grain cores, whereas As, Au, and Cu are enriched in irregularly shaped intermediate growth zones; Mo also appears weakly concentrated in these intermediate zones, as well as in U585EX315. With the exception of weak anomalies of Ni, Tl and Co defining narrow, regular (cubic) growth zones, the outer grain-rim areas beyond the irregularly shaped intermediate growth zones do not usually display trace-element zonation.

## Electrum

Initial EMPA-WDS analyses of electrum from the different mineralized VOK vein stages and substages identified an apparently regular and systematic variation in the Au:Ag ratio of the mineral with vein type. A significant number ( $n = 24$ ) of new samples have been analyzed since this finding was first published (McLeish et al., 2017). They show that the variation in electrum chemistry between vein types initially documented holds true across the VOK. New samples were collected from each vein type, based on the nature and abundance of electrum mineralization present. Specific emphasis was placed on selecting samples from the  $Vn_2$ -type veins, which were not analyzed during the initial study.

A large number of EMPA-WDS analyses of electrum were performed at the McGill University Electron Microprobe Laboratory and the joint University of Ottawa–Canadian Museum of Nature MicroAnalysis Laboratory, using JEOL 8900 and JEOL 8230 SuperProbe instruments, respectively. Both instruments are equipped with five X-ray wavelength-dispersive spectrometers and, with limited exceptions, identical operating conditions were used at both

facilities. Electrum grains were quantitatively analyzed for Ag ( $L\alpha$ ), Au ( $M\alpha$ ), Hg ( $L\alpha$  in Montréal;  $M\beta$  in Ottawa) and Te ( $L\beta$ ) using the following synthetic and natural standards: Au60Ag40 alloy (Au and Ag), cinnabar (Hg) and native Te (Te in Montréal;  $Sb_2Te_3$  in Ottawa). Microbeam analyses were performed using a beam energy of 20 keV, a 40° takeoff angle, a 5  $\mu$ m beam diameter and a 30 nA beam current (40 nA current in Ottawa). Duplicate EMPA-WDS spot tests were done on selected electrum grains at both facilities and no significant difference in results was observed.

Gold and silver results from the EMPA-WDS analyses of electrum are shown, together with those from McLeish et al. (2017), in Figure 6. The Au:Ag ratio of the electrum appears to vary considerably with vein type, and no significant variation in the Au:Ag ratio of electrum was observed within individual samples. Analyses were taken across electrum grains (rim-core-rim) for both quartz-carbonate-matrix-hosted and pyrite-inclusion-hosted electrum, with no obvious Au:Ag differences observed. No Te was detected in the electrum; trace levels of mercury (<1.4 wt. %) were found in electrum samples with a high Ag content (40–60 wt. %) from  $Vn_2$  veins. The regular, systematic variation in the Au:Ag ratio of the electrum with vein type was confirmed, with some overlap observed between vein types. Two  $Vn_2$  samples in which electrum occurs in textural equilibrium with galena and sphalerite (SU-312 and SU-580) yielded Au values significantly lower than in  $Vn_2$  veins where no textural equilibrium was observed between electrum and base-metal sulphide mineralization. Initial three-dimensional modelling of the electrum chemistry results show that there is no significant spatial control on electrum chemistry.

## Summary and Future Work

The petrographic and mineral chemistry results presented here indicate that the Brucejack deposit was formed from multiple, possibly long-lived mineralizing events, which likely originated from at least two chemically and temporally distinct hydrothermal systems. The finding of high-grade invisible Au mineralization in As-rich growth zones of pyrite crosscut by electrum demonstrates that a significant Au mineralization event predated the hydrothermal activity responsible for the three generations of epithermal quartz-carbonate-electrum veins ( $Vn_1$ – $Vn_3$ ). Furthermore, evidence of pre-electrum, post-auriferous-pyrite deformation indicates that the pyrite-hosted Au and electrum mineralization were separated by a deformation event of presently unknown extent.

Preliminary petrographic observations suggest that the older, invisible Au-hosting pyrite within the ore-stage veins of the VOK was likely inherited from the adjacent phyllically altered wallrocks. If the phyllic alteration af-

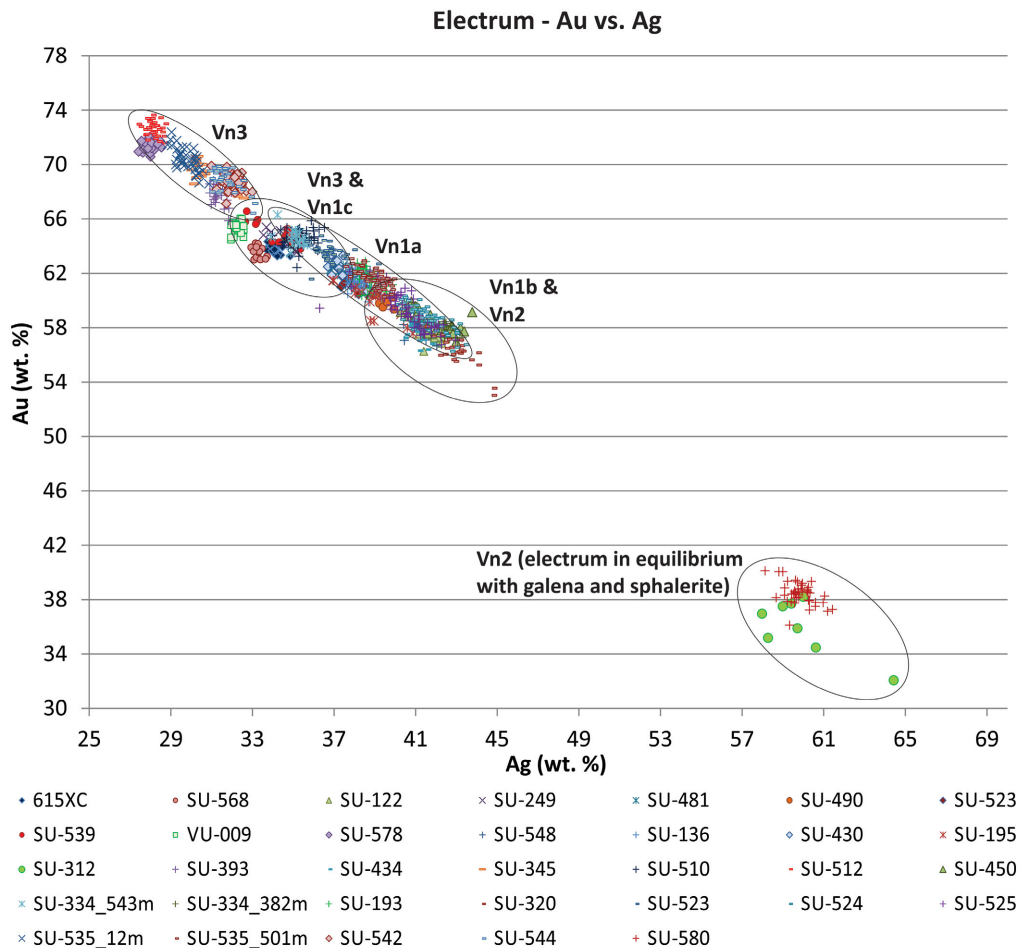


**Figure 6:** Gold and silver concentrations in electrum from the Valley of the Kings zone at the Brucejack deposit, based on EMPA-WDS analyses. See text for discussion.

fecting the VOK wallrocks is genetically related to the broader phyllic-alteration halo surrounding the older Kerr-Sulphurets-Mitchell and Snowfield porphyry deposits, as has been suggested from regional mapping (e.g., Nelson and Kyba, 2014), the invisible pyrite-hosted Au mineralization identified here may be the product of an approximately 8–10 m.y. older, magmatic-hydrothermal mineralizing event. The implications of such a genetic model, if correct, are potentially profound considering the widespread nature and strength of pyrite alteration/mineralization in phyllically altered country rocks of the VOK. For example, this model would suggest that 1) the electrum-hosting epithermal veining alone is not sufficient to account for the 8.7 million ounce Au reserve at Brucejack; and 2) the broad swath of phyllically altered country rocks in the vicinity of the VOK have the potential to, on their own, host possibly significant refractory Au mineralization.

Mineral chemistry and petrographic investigations will continue, and the fluid-inclusion and thermodynamic-modelling work described in the initial *Summary of Activi-*

*ties* paper (McLeish et al., 2017) will begin, in order to further test hypotheses advanced in that paper and to look for other insights into the origin and physicochemical evolution of the deposit. A major thrust of the research during the coming year will be to determine the reason for the extraordinarily high Au concentrations in the Brucejack deposit. To this end, work will build on the observations of Harrichhausen (2016) and Harrichhausen et al. (2016) of Au-Ag nanoparticles in relict amorphous silica-hosted electrum dendrites at Brucejack, by conducting a comprehensive high-resolution (nano-scale) transmitted electron microscopic (TEM) examination of electrum in the deposit. If it can be demonstrated that much of the electrum was initially nanoparticulate, this could eliminate the dependence on simple solubility and point to colloidal processes (mechanical transport) as a potentially important means of Au hyperenrichment (cf. Williams-Jones et al., 2009).

### Acknowledgments

Major funding for this project is being provided by the Natural Sciences and Engineering Research Council of Canada

(NSERC) and Pretium Resources Inc. The authors thank O. Vasyukova for providing a careful and constructive review of this paper. The lead author also thanks Geoscience BC and the Society of Economic Geologists (SEG) for their financial support through the Geoscience BC Scholarship and SEG Student Research Grant programs, respectively. Lastly, the authors gratefully acknowledge the logistical and accommodation support generously provided by Pretium during the summer field season.

## References

- Alldrick, D.J. (1993): Geology and metallogeny of the Stewart mining camp, northwestern British Columbia; BC Ministry of Energy, Mines and Petroleum Resources, BC Geological Survey, Bulletin 85, 105 p.
- Anderson, R.G. (1993): A Mesozoic stratigraphic and plutonic framework for northwestern Stikinia (Iskut River area), northwestern British Columbia, Canada; *in* Mesozoic Paleogeography of the Western United States, II, G.C. Dunne and K.A. McDougall (ed.), Society of Economic Paleontologists and Mineralogists, Pacific Section, Los Angeles, California, p. 477–494.
- BC Geological Survey (2017): MINFILE BC mineral deposits database; BC Ministry of Energy, Mines and Petroleum Resources, BC Geological Survey, URL <<http://minfile.ca/>> [November 2017].
- Board, W.S. (2014): Brucejack geology summary; Pretium Resources Inc., URL <[http://s1.q4cdn.com/222336918/files/doc\\_downloads/geology/2013429\\_Geology\\_for\\_web\\_site\\_APRIL2013\\_WSB.pdf](http://s1.q4cdn.com/222336918/files/doc_downloads/geology/2013429_Geology_for_web_site_APRIL2013_WSB.pdf)> [November 2016].
- Board, W.S. and McNaughton, K.C. (2013): The Brucejack high-grade gold project, northwest British Columbia, Canada; *in* Proceedings of NewGenGold Conference, November 26–27, 2013, Perth, Australia, p. 177–191.
- Bridge, D.J. (1993): The deformed Early Jurassic Kerr copper-gold porphyry deposit, Sulphurets gold camp, northwestern British Columbia; M.Sc. thesis, The University of British Columbia, Vancouver, BC, 303 p.
- Febbo, G.E., Kennedy, L.A., Savell, M., Creaser, R.A. and Friedman, R.M. (2015): Geology of the Mitchell Au-Cu-Ag-Mo porphyry deposit, northwestern British Columbia, Canada; *in* Geological Fieldwork 2014, BC Ministry of Energy, Mines and Petroleum Resources, BC Geological Survey, Paper 2015-1, p. 59–86.
- Ghaffari, H., Huang, J., Hafez, S.A., Pelletier, P., Armstrong, T., Brown, F.H., Vallat, C.J., Newcomen, H.W., Weatherly, H., Wilchek, L. and Mokos, P. (2012): Technical report and updated preliminary economic assessment of the Brucejack project; NI 43-101 report by Tetra Tech, Wardrop, Rescan, PE Mining, Geospark and AMC Mining, 327 p.
- Greig, C.J. and Brown, D.A. (1990): Geology of the Stikine River–Yehiniko Lake area, northwestern British Columbia; Geological Association of Canada–Mineralogical Association of Canada, Joint Annual Meeting, Program with Abstracts, v. 15, p. A51.
- Harrichhausen, N.J. (2016): Role of colloidal transport in the formation of high-grade gold veins at Brucejack, British Columbia; Ph.D. thesis, McGill University, Montréal, Quebec, 123 p.
- Harrichhausen, N.J., Rowe, C.D., Board, W.S. and Greig, C.J. (2016): Relationship between amorphous silica and precious metals in quartz veins: examples from Brucejack, British Columbia and Dixie Valley, Nevada; Association for Mineral Exploration (AME) Roundup, conference poster, URL <[http://www.geosciencebc.com/i/pdf/Roundup2016/2016%20poster\\_Harrichhausen.pdf](http://www.geosciencebc.com/i/pdf/Roundup2016/2016%20poster_Harrichhausen.pdf)> [November 2016].
- Johnston, S.T. (2008): The Cordilleran ribbon continent of North America; Annual Review of Earth and Planetary Sciences, v. 36, p. 495–530.
- Kirkham, R.V. and Margolis, J. (1995): Overview of the Sulphurets area, northwestern British Columbia; *in* Porphyry Deposits of the Northwestern Cordillera of North America, T.G. Schroeter (ed.), Canadian Institute of Mining, Metallurgy and Petroleum, Special Volume 46, p. 473–508.
- Logan, J.M. and Mihalynuk, M.G. (2014): Tectonic controls on Early Mesozoic paired alkaline porphyry deposit belts (Cu-Au ± Ag-Pt-Pd-Mo) within the Canadian Cordillera; Economic Geology, v. 109, p. 827–858.
- Macdonald, A.J., Lewis, P.D., Thompson, J.F.H., Nadaraju, G., Bartsch, R., Bridge, D.J., Rhys, D.A., Roth, T., Kaip, A., Godwin, C.I. and Sinclair, A.J. (1996): Metallogeny of an Early to Middle Jurassic arc, Iskut River area, northwestern British Columbia; Economic Geology, v. 91, p. 1098–1114.
- Margolis, J. (1993): Geology and intrusion related copper-gold mineralization, Sulphurets, British Columbia; Ph.D. thesis, University of Oregon, Eugene, Oregon, 289 p.
- Marsden, H. and Thorkelson, D.J. (1992): Geology of the Hazelton Volcanic Belt in British Columbia: implications for the Early to Middle Jurassic evolution of Stikinia; Tectonics, v. 11, p. 1266–1287.
- McLeish, D.F. (2013): Structure, stratigraphy, and U-Pb zircon-titanite geochronology of the Aley carbonatite complex, northeast British Columbia: evidence for Antler-aged orogenesis in the Foreland Belt of the Canadian Cordillera; M.Sc. thesis, University of Victoria, Victoria, BC.
- McLeish, D.F., Williams-Jones, A.E. and Board, W.S. (2017): Nature and origin of the Brucejack high-grade epithermal gold deposit, northwestern British Columbia (NTS 104B); *in* Geoscience BC Summary of Activities 2016, Geoscience BC, Report 2017-1, p. 223–231, URL <[http://www.geosciencebc.com/i/pdf/SummaryofActivities2016/SoA2016\\_McLeish.pdf](http://www.geosciencebc.com/i/pdf/SummaryofActivities2016/SoA2016_McLeish.pdf)> [October 2017].
- Monger, J.W.H., Wheeler, J.O., Tipper, H.W., Gabrielse, H., Harms, T., Struik, L.C., Campbell, R.B., Dodds, C.J., Gehrels, G.E. and O’Brien, J. (1991): Upper Devonian to Middle Jurassic assemblages; Chapter 8 *in* Geology of the Cordilleran Orogen in Canada, H. Gabrielse and C.J. Yorath (ed.), Geological Survey of Canada, Geology of Canada, No. 4, p. 281–328.
- Nelson, J. and Kyba, J. (2014): Structural and stratigraphic control of porphyry and related mineralization in the Treaty Glacier–KSM–Brucejack–Stewart trend of western Stikinia; *in* Geological Fieldwork 2013, BC Ministry of Energy, Mines and Petroleum Resources, BC Geological Survey, Paper 2014-1, p. 111–140.
- Reich, M., Kesler, S.E., Utsunomiya, S., Palenik, C.S., Chrysosoulis, S.L. and Ewing, R.C. (2005): Solubility of gold in arsenian pyrite; *Geochimica et Cosmochimica Acta*, v. 69, p. 2781–2796.
- Tombe, S.P. (2015): Tectonomagmatic setting of the Sulphurets Cu-Au porphyry-epithermal district, northwestern British

Columbia. M.Sc. thesis; University of Alberta, Edmonton, AB, 178 p.

Tombe, S.P., Greig, C.J., Board, W.S., Richards, J.P., Friedman, R.M. and Creaser, R.A. (2014): The Brucejack porphyry-related epithermal Au deposit, northwestern British Columbia; PDAC-CMIC-SEG Canada Student Minerals Colloquium, conference abstracts; URL <[\[footprints.ca/smc/files/2014/Tombe\\\_2014SMC\\\_British%20Columbia\\\_Porphyry\\\_Gold%20Silver%20Brucejack.pdf\]\(http://footprints.ca/smc/files/2014/Tombe\_2014SMC\_British%20Columbia\_Porphyry\_Gold%20Silver%20Brucejack.pdf\)> \[November 2016\].](http://cmic-</a></p></div><div data-bbox=)

Williams-Jones, A.E., Bowell, R.J. and Migdisov, A.A. (2009): Gold in solution; Elements, v. 5, p. 281–287. doi:10.2113/gselements.5.5.281